THE JOURNAL OF PHYSICAL CHEMISTRY A

Article

pubs.acs.org/JPCA



# Spectroscopy of Lithium Atoms and Molecules on Helium Nanodroplets

Florian Lackner,* Johannes Poms, Günter Krois, Johann V. Pototschnig, and Wolfgang E. Ernst*

Institute of Experimental Physics, Graz University of Technology, Petersgasse 16, A-8010 Graz, Austria/EU

**ABSTRACT:** We report on the spectroscopic investigation of lithium atoms and lithium dimers in their triplet manifold on the surface of helium nanodroplets ($He_N$). We present the excitation spectrum of the 3p ← 2s and 3d ← 2s two-photon transitions for single Li atoms on $He_N$. The atoms are excited from the 2S(Σ) ground state into Δ, Π, and Σ pseudodiatomic molecular substates. Excitation spectra are recorded by resonance enhanced multiphoton ionization time-of-flight (REMPI-TOF) mass spectroscopy, which allows an investigation of the exciplex ($Li^*–He_m$, $m$ = 1−3) formation process in the Li−$He_N$ system. Electronic states are shifted and broadened with respect to free atom states, which is explained within the pseudodiatomic model. The assignment is assisted by theoretical calculations, which are based on the Orsay−Trento density functional where the interaction between the helium droplet and the lithium atom is introduced by a pairwise additive approach. When a droplet is doped with more than one alkali atom, the fragility of the alkali−$He_N$ systems leads preferably to the formation of high-spin molecules on the droplets. We use this property of helium nanodroplets for the preparation of Li dimers in their triplet ground state ($1^3\Sigma_u^+$). The excitation spectrum of the $2^3\Pi_g(\nu' = 0–11) \leftarrow 1^3\Sigma_u^+(\nu'' = 0)$ transition is presented. The interaction between the molecule and the droplet manifests in a broadening of the transitions with a characteristic asymmetric form. The broadening extends to the blue side of each vibronic level, which is caused by the simultaneous excitation of the molecule and vibrations of the droplet (phonons). The two isotopes of Li form $^6Li_2$ and $^7Li_2$ as well as isotope mixed $^6Li^7Li$ molecules on the droplet surface. By using REMPI-TOF mass spectroscopy, isotope-dependent effects could be studied.

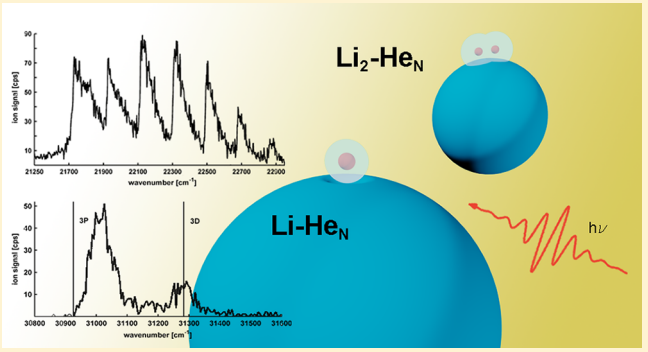


## INTRODUCTION

Helium nanodroplets ($He_N$) have attracted strong interest as superfluid nanocryostats for the efficient preparation of tailored molecules and clusters at ultracold temperatures.[1,2] The spectroscopy of atoms on/in helium nanodroplets gives insight into the nature of interactions between a nanosized superfluid and single atoms. Moreover, the special properties of helium nanodroplets enable the formation of tailored molecules and offer a possibility to study complexes that can not, or only with great expense, be produced in the gas phase or in molecular beam experiments. An example is the preparation of alkali (Ak) metal dimers[3] and trimers[4] in their weakly bound high-spin configuration (triplet and quartet states, respectively) or even high spin clusters[5,6] at low temperatures (0.37 K[7]).

The lowest electronic transitions (D1 and D2 lines) in Ak atoms on the surface of helium nanodroplets are well characterized.[8−14] The D1 and D2 lines of Li atoms on the surface[15] of $He_N$ are an exception among the Ak−$He_N$ systems because their main absorption peak is lower in energy than the free atom transition. This red-shift has its origin in bound−bound transitions from the ground state into the two 2P(Π) states.[14] While excitation spectra of Rydberg states for Na,[16,17] Rb,[18−22] and Cs[18,19,23] have been reported, less work has been done on the characterization of K−$He_N$ and Li−$He_N$. Besides the D1 and D2 lines, only the 5p ← 4s transition in K−$He_N$[18] and the 3s ← 2s transition in Li−$He_N$[24] have been investigated.

For the assignment of excited states of Ak atoms on $He_N$, we use the pseudodiatomic model (Hund's *case a* notation is appropriate[18,19]). Because of the presence of the droplet, the symmetry of the atomic system is broken and only the projection of the atomic orbital angular momentum L onto the intermolecular axis (i.e., Λ), which is defined by the connection between the droplet center and the Ak nucleus, remains a conserved quantity. In the case of Li, spin−orbit (SO) splitting can be neglected (e.g., SO splitting for the 2P state: 0.34 $cm^{-1}$[25]). For two-photon excitations, transitions from the Li−$He_N$ 2S(Σ) ground state into Δ, Π, and Σ molecular substates are allowed.

The fragility of systems formed by helium nanodroplets with molecules on their surface enhances the formation of weakly bound complexes because the binding energy, which is gained during the formation of the molecule, is released into the droplet. This excess energy could destroy the complex formed

**Special Issue:** Curt Wittig Festschrift

**Received:** March 27, 2013
**Revised:** July 29, 2013
**Published:** July 29, 2013

   dx.doi.org/10.1021/jp4030238 | J. Phys. Chem. A 2013, 117, 11866−11873

by the molecule and the droplet. Hence, the weakly bound alkali dimers in the triplet manifold have a higher probability of survival than the singlet molecules, and the helium droplets act as a filter for Ak dimers in the triplet manifold. Triplet bands of $Na_2$,[3,4] $K_2$,[4,26] $Rb_2$,[26−28] and $Cs_2$[29] have been studied in detail. For $Li_2$ on $He_N$, only the $1^3\Pi_g \leftarrow 1^3\Sigma_u^+$ transition, which is a bound-free transition, has been reported so far.[4] The orientation of the ground state Li dimers for the two different spin configurations ($^1\Sigma_g^+$ and $^3\Sigma_u^+$ state) with respect to the droplet surface has been investigated theoretically for small $He_N$ (for $N$ up to 30), where it was found that the singlet molecule is perpendicular and the triplet one is oriented parallel to the droplet's surface.[30] In contrast to the $Li_2$−$He_N$ system, triplet bands of free $Li_2$ molecules have been studied extensively experimentally[31] as well as theoretically.[32] The most accurate experimental data have been recorded by perturbation facilitated optical−optical double resonance (PFOODR) spectroscopy.[31] This allows a detailed comparison between molecules on $He_N$ and free molecules, which reveals insight into the interaction between the superfluid droplet and the molecule on its surface.

In the first part of this article, we report on the investigation of the two-photon 3p ← 2s and 3d ← 2s transitions in Li−$He_N$ by resonance enhanced multiphoton ionization time-of-flight (REMPI-TOF) spectroscopy. Pseudodiatomic molecular substates are identified on the basis of the observed abundance of exciplexes because the exciplex formation process depends on Λ of the molecular substate. Calculations based on a pairwise additive approach support our assignment. In the second part of this article, we report on the investigation of the $2^3\Pi_g \leftarrow 1^3\Sigma_u^+$ transition of the Li dimer on $He_N$. Vibronic states could be resolved and the low mass of the Li atom in combination with the REMPI-TOF technique allows to study the band for all three Li isotopomers, $^6Li_2$, $^7Li_2$, and $^6Li^7Li$, as well as an investigation of their interaction with the droplet.

## EXPERIMENTAL SECTION

A detailed description of the experimental setup can be found in refs 33 and 34. High purity helium gas is cooled down to a temperature of $T_0$ = 15 K and expanded through a $d_0$ = 5 μm nozzle under a pressure of $p_0$ = 60 bar into vacuum. These conditions lead to a subcritical supersonic jet expansion of the He gas and consequently to the formation of helium droplets, where the droplet size follows a logarithmic normal distribution. The source conditions lead to a distribution maximum ($\hat{N}_{p0,T0}$) at $\hat{N}_{60,15}$ = 6000 He atoms,[35,36] which corresponds to a droplet radius of $\hat{R}_{60,15}$ = 40 Å. After production, the helium droplet beam is guided into another vacuum chamber where it is doped with Li by passing through a resistively heated pickup cell. The pickup statistic obeys a Poisson distribution.[35] The process depends on the vapor pressure within the pickup cell, which is controlled by the cell temperature. At the used temperature of $T \cong$ 350 °C, Li atoms as well as Li dimers are present on the droplets.

The excitation spectra have been obtained by resonance enhanced multiphoton ionization time-of-flight (REMPI-TOF) spectroscopy. A tunable pulsed dye laser (Lambda Physik FL 3002) is used to access Li−$He_N$ and $Li_2$−$He_N$ transitions. To cover the spectral range, three different laser dyes have been used. The $Li_2$−$He_N$ dimer spectrum has been obtained by resonant two-photon ionization, using Coumarin 2 (0.3 mJ) and Stilbene 3 (0.5 mJ). The Li−$He_N$ complexes have been excited via a two-photon scheme (without a resonant intermediate state) with DCM (5.2 mJ) and ionized with a fraction (0.6 mJ) of the XeCl pump laser radiation (Radiant Dyes RD-EXC-200 XeCl laser, 26 ns pulse duration, 100 Hz).

## RESULTS

**Spectroscopy of Li Atoms on $He_N$.** In this section, we discuss the two-photon 3p ← 2s and 3d ← 2s transitions in Li−$He_N$. Because of the small size of the Li ion core, states with $l$ > 0 lie energetically very close together in the lithium atom (these states have a core nonpenetrating character[37]). Only the $n$S states are significantly shifted with respect to the hydrogenic term energy. Note that because of the $l < n$ condition for the orbital angular momentum quantum number $l$ the 3D state investigated here is a special case among the $n$D Li−$He_N$ Rydberg series because it does not overlap with an F state.

The two-photon excitation spectrum of the 3p ← 2s and 3d ← 2s transitions in Li−$He_N$ is depicted in Figure 1. The ion

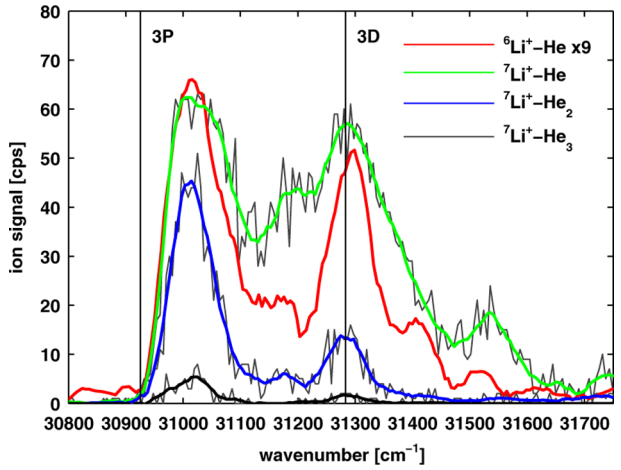


**Figure 1.** Two-photon excitation spectrum of Li−$He_N$. The spectrum is obtained by monitoring the $^6Li^+$−He (red, ×9, smoothed signal only), $^7Li^+$−He (green), $^7Li^+$−$He_2$ (blue), and $^7Li^+$−$He_3$ (black) ion yield as a function of the excitation laser wavenumber (multiplied by two) with a time-of-flight mass spectrometer. The 3P and 3D free atom states at 30 925 cm$^{-1}$ and 31 283 cm$^{-1}$[25] are shown as vertical black lines.

yield for $^6Li^+$−He (red, ×9, smoothed signal only), $^7Li^+$−He (green), $^7Li^+$−$He_2$ (blue), and $^7Li^+$−$He_3$ (black) is monitored as a function of the laser wavenumber, which is multiplied by two to account for the absorption of two photons. The vertical lines represent the positions of the free atom 3P and 3D states. The bare $Li^+$ atom signal is not shown because the high photon density also excites the strongly repulsive blue wing of the 2P(Σ) state[8] (one-photon transition) and ionizes desorbed Li 2P atoms, causing a large background signal. The $Li^+$−$He_m$ ($m$ > 0) spectra are free from this background signal. The resonance with the intermediate 2P(Σ) state enhances the two-photon transition, similar to the two-photon transition studied for Rb−$He_N$ in ref 18.

While for the Li−$He_N$ 3s ← 2s transition in ref 24 only bare lithium ions were detected, the excitation of states with Λ > 0 leads to the formation of exciplexes (Ak*−$He_m$).[38] The $Li^+$−$He_m$ ion signals show the same structure as has been observed for heavier Ak atoms[17,18,20,23] and can be explained within the pseudodiatomic model. In this picture, the 3P state splits into a Π and Σ component (neglecting spin−orbit effects). It is known that upon excitation of the Ak−$He_N$ system into Σ


dx.doi.org/10.1021/jp4030238 | J. Phys. Chem. A 2013, 117, 11866−11873

states a large fraction of the atoms desorb without attached helium atoms. In contrast, the ionization via states with $\Lambda > 0$ is always accompanied by an abundance of Ak−$He_m$ ($m > 0$) complexes in the time-of-flight mass spectra. Hence, we attribute the pronounced peak at (31 016 ± 2) $cm^{-1}$, full width at half-maximum (fwhm) = (43 ± 3) $cm^{-1}$ (as monitored on the $^7Li^+$−$He_2$ mass) to the 3P(Π) state. We call this approach for the assignment of excited states based on the exciplex formation process the "exciplex approach" in the following. In contrast, the signal in between the 3P(Π) and the 3D line is only visible in the $Li^+$−He ion signal; hence, we attribute this part of the spectrum to the onset of the 3P(Σ) state. The structure of the signal, which correlates to the 3D molecular substates, is similar to the signal obtained for the Rb−$He_N$ system in ref 20. The state related to the peak at (31 278 ± 5) $cm^{-1}$, fwhm = (52 ± 7) $cm^{-1}$ (as monitored on the $^7Li^+$−$He_2$ mass) is accompanied with a high probability for the formation of exciplexes. Hence, we assign this peak to the 3D (Δ) state. It is remarkable that this state appears almost unshifted with respect to the free atom transition at 31 283 $cm^{-1}$.[25] Considering the depth of the Li−$He_N$ 2S(Σ) ground state potential of ∼10 $cm^{-1}$, which has to be taken into account when excitation spectra are compared to free atom transitions, the 3D(Δ) potential has a binding character and its minimum lies about (−15 ± 7) $cm^{-1}$ below the asymptotic 3D energy. This demonstrates a weak attractive interaction of the Li atom in the 3D(Δ) state with the droplet. Similar signals have been observed in ref 17 for the Na−$He_N$ 4P ← 3S and 4D ← 3S transitions, which compare to the presented Li−$He_N$ transitions. Therein, increased exciplex formation upon excitations into states associated with high Λ was observed close by the free Na atom lines. In the $^7Li^+$−He ion signal, the blue shoulder of the 3D(Δ) peak extends to much higher wavenumbers than in the $^7Li^+$−$He_2$ detected spectrum, and it is followed by a second peak at (31 536 ± 10) $cm^{-1}$, which we attribute either to a part of the 3D (Π) or (Σ) state.

To simulate the spectra, we use the Orsay−Trento density functional[39] as implemented in the code by F. Dalfovo, with modifications by K. K. Lehmann and R. Schmied.[40−42] The interaction between the helium droplet and the alkali atom is introduced by a pairwise additive (PWA) approach. To obtain the radial density profile of the ground state, the lithium−helium potential of Patil[43] is used. For the excited states, the curves of Pascale represent the set of Li*−He interactions of the electronic states relevant for this work.[44,45] An effective coordinate $z_{Li}$ is introduced as the distance between the center of mass of the droplet and the lithium atom. By convoluting the density with the above pair potentials, we obtain the pseudodiatomic potentials shown in Figure 2. We accounted for the correct projection of the angular momentum on the helium−lithium axis by means of Wigner rotation matrices, following ref 13 and transforming the Hamiltonian in a diagonal shape. Spin−orbit coupling can be neglected, as the interaction with the droplet is much larger. In the frozen droplet picture, assuming a fast desorption of the lithium atom upon excitation,[24] Franck−Condon factors (FCFs) are calculated with the help of BCONT 2.2 by LeRoy[46] for bound-free transitions of the pseudodiatomic molecule. The majority of the Li−$He_N$ systems are in their vibronic ground state ($\nu = 0$) before the excitation.

The calculated FCFs are shown in Figure 3. It can be seen that our approach overestimates the blue shift of the excited states. Such large blue shifts on the order of several thousand

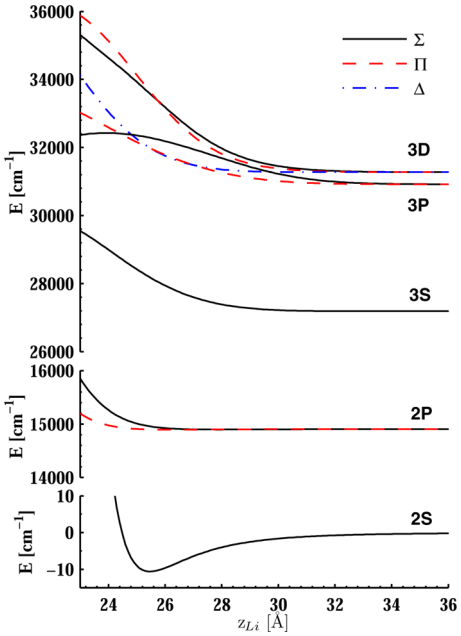


**Figure 2.** Calculated pseudodiatomic potential energy curves for a Li−$He_{1000}$ droplet. The Li atomic states are used as a label on the right side for large distances $z_{Li}$. Depending on the angular momentum the curve splits into Σ(Λ = 0) states (solid line), Π(Λ = 1) states (dashed), and Δ(Λ = 2) states (dashed−dotted). Note the different ordinate scales.

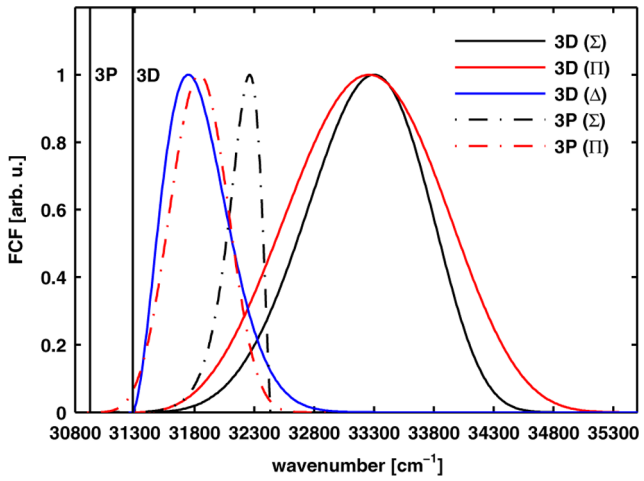


**Figure 3.** Calculated Franck−Condon factors (scaled to one) as obtained with the PWA approach as described in the text. Full lines represent the molecular substates arising from the 3D state, and dashed lines represent the 3P substates.

wavenumbers have already been observed for calculations of excited states of Na−$He_N$ in ref 17, where it was shown that the PWA approach works best at states with low principal quantum number $n$. In addition to the PWA approach, for Na−$He_N$ a perturbative configuration interaction (PCI) approach was used, where the helium dopant interaction is introduced by a perturbation rather than a pair potential. The PCI model shows a better agreement with the experimental spectra than the PWA approach; unfortunately, this model is not yet parametrized for lithium. Although our potential energy curves (see Figure 2) for the 2S(Σ), 2P(Π,Σ), and 3S(Σ) reproduce the results of other calculations,[13,24] the spectrum for the 3P and 3D states is far off the experimental one. However, the calculated theoretical


dx.doi.org/10.1021/jp4030238 | J. Phys. Chem. A 2013, 117, 11866−11873

spectrum for the transition from the ground state into the 3S(Σ) state has a maximum at ∼27 880 $cm^{-1}$, which matches the experimental peak maximum (∼27 820 $cm^{-1}$) very well as can be seen from Figure 4 in ref 24. The difference between

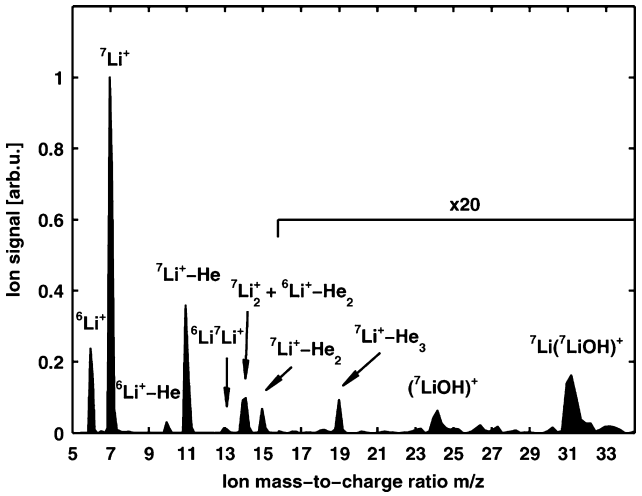


**Figure 4.** Time-of-flight mass spectrum as obtained while the laser is scanned across the two-photon transitions, which is shown in Figure 1. The most intense ion signal is detected for $^6Li$ and $^7Li$ ions. Peaks in steps of 4 amu are related to Li ions with attached helium atoms. In addition to Li dimers, which are formed on the droplets, also complexes of Li, $Li_2$, and residual water, which is present in the vacuum chamber, are observed in the mass spectrum.

theory and experiment for the 3P and 3D spectra is expected to some extent due to several approximations in the PWA approach: (i) the ground state helium density is assumed to be maintained during the excitation (frozen droplet approximation), (ii) interactions between 3P and 3D states are not included, but in the case of Li the states lie relatively close, and (iii) the approach rests on the potentials calculated by Pascale.[44,45] Despite the fact that Pascale's potentials have been leading to numerous fruitful results, they might be not as accurate as modern calculations.[47]

The above discussion reveals that a more sophisticated approach is needed to describe higher excited states of Li−$He_N$ accurately. Different approaches have been presented recently[48] where the best results for Li−$He_N$ have been obtained with the methods developed by the Barranco group.[14,24] However, the energetic ordering as described above for the 3P(Π), 3P(Σ), 3D(Δ), 3D(Π), and 3D(Σ) states is reproduced by our calculations. According to the PWA approach, the 3P(Π) state lies energetically lower than the 3P(Σ) state, and the 3D(Δ) state is the energetically lowest among the three 3D molecular substates, which is in agreement with our assignment within the exciplex approach. Despite the differences between calculation and experiment, we think that the expected energetic ordering of excited states confirms our interpretation within the exciplex approach.

For the 3s ← 2s transition, an isotope shift for the two different Li isotopes has been observed.[24] As can be seen from the excitation spectrum in Figure 1, we do not observe a significant isotope effect within the accuracy of our data.

Figure 4 shows the time-of-flight mass spectrum as obtained, while the laser is scanned across the two-photon transitions (Figure 1). The highest signal is detected at the mass-to-charge ratio $m/z$ corresponding to bare $^6Li$ and $^7Li$ ions. The intensity of the peaks reflects the natural abundance of the two Li isotopes ($^6Li$, 7.4%; $^7Li$, 92.6%). These two Li mass peaks are followed by peaks originating from Li−He, Li−$He_2$, and Li−$He_3$ in steps of 4 amu ($^4He$). Because of the high photon density and the presence of the 308 nm light, Li dimers ($^6Li_2$, $^6Li^7Li$, and $^7Li_2$) are also observed in the mass spectrum. At higher $m/z$ ratios (for $m/z$ > 16 the signal is multiplied by a factor of 20), two prominent peaks are observed. These peaks are related to residual water, which was present in our chamber during the experiment. We attribute the peaks at $m/z$ = 24 and $m/z$ = 31 to the products of an oxidative hydrolysis of $^7LiOH$ and $^7Li(^7LiOH)$, respectively, which are produced upon a reaction with water in the helium droplet.[49] Because of the resonant excitation of an intermediate state, the reaction may be enhanced by the present laser photons. This could explain the absence of a prominent peak corresponding to the weakly bound $^7Li$−$H_2O$ ($m/z$ = 25) van der Waals complex, which is in contrast to the findings in ref 49. We find no evidence for the

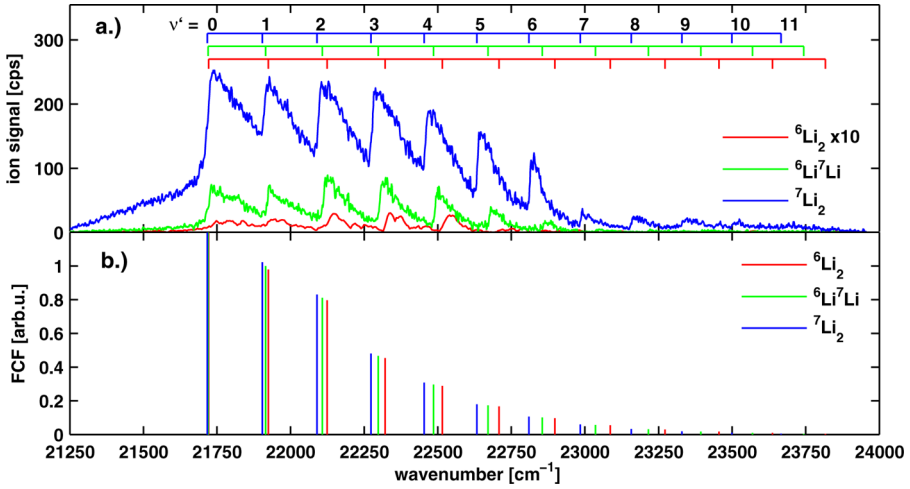


**Figure 5.** Excitation spectrum of the $2^3\Pi_g$ ($\nu'$) ← $1^3\Sigma_u^+$ ($\nu''$ = 0) triplet transitions of Li dimers on the surface of helium nanodroplets (a). The spectrum is obtained by resonant two-photon ionization spectroscopy. The spectra of all three isotopomers $^6Li_2$ (red), $^6Li^7Li$ (green), and $^7Li_2$ (blue) are shown. Calculated Franck−Condon factors are shown (in arbitrary units) as vertical bars and scaled to the $\nu'$ = 1 peak (b).


dx.doi.org/10.1021/jp4030238 | J. Phys. Chem. A 2013, 117, 11866−11873

Table 1. Molecular Parameters for $^6Li_2$, $^6Li^7Li$, and $^7Li_2$ on the Surface Helium Nanodroplets[a]

| | $^7Li_2$ on $He_N$ | $^7Li_2$, Li et al.[61] | $^6Li^7Li$ on $He_N$ | $^6Li^7Li$ calcd | $^6Li_2$ on $He_N$ | $^6Li_2$, Xie and Field[58] |
|---|---|---|---|---|---|---|
| $T$ | 21623 (9) | | 21621 (6) | | 21601 (44) | |
| $T_e$ | 29837 (9) | 29844.7 | 29836 (6) | | 29817 (44) | 29840.5 |
| $\omega_e$ | 189.7 (4.7) | 188.66 | 201 (3.3) | 196.36 | 215 (41) | 204.2 |
| $\omega_e x_e$ | 1.15 (0.5) | 1.20 | 1.7 (0.4) | 1.29 | 2.6 (8) | 1.37 |

[a]Only vibronic transitions where the rising edge could be clearly identified are included in the fit procedure $^7Li_2$, $\nu' = 0-8$; $^6Li^7Li$, $\nu' = 0-8$; $^6Li_2$, $\nu' = 0-4$. Parameters are given in $cm^{-1}$, and one standard deviation uncertainties are given in parentheses. Parameters for $^6Li^7Li$ are calculated from the parameters given by Li et al.[61]

formation of Li clusters (i.e., $Li_{m>2}$) at our source conditions. This is in agreement with other experiments as discussed in ref 5. The absence of these complexes is related to the high formation energies of lithium clusters,[50] which are significantly higher than those of the heavier Ak clusters and have been investigated in detail on/in helium nanodroplets.[5,6,51,52] We think that the production of Li clusters will require larger helium droplets ($N > 10^5$) produced by source conditions with lower temperatures in the supercritical expansion regime.

**Spectroscopy of Li Dimers on $He_N$.** The excitation spectrum of Li dimers in the range between 21 250 and 24 000 $cm^{-1}$ is shown in Figure 5a. The spectrum was obtained by resonant two-photon ionization spectroscopy. The observed vibronic transitions are identified as $2^3\Pi_g$ ($\nu'$) ← $1^3\Sigma_u^+$ ($\nu'' = 0$). The ion yield for $m/z$ = 12 ($^6Li_2$), 13 ($^6Li^7Li$), and 14 ($^7Li_2$) was monitored as a function of the dye laser wavenumber. Hence, the excitation spectra of all three isotopomers are observed. The composition of the molecules on the droplets is 85.71% $^7Li_2$, 13.71% $^6Li^7Li$, and 0.55% $^6Li_2$. Because of the low abundance of $^6Li_2$, the ion signal obtained for $^6Li_2$ is very weak and was smoothed and multiplied by a factor of 10. The spectrum comprises a series of progressive vibrational bands, which can be followed, in the case of $^7Li_2$, from $\nu' = 0$ up to $\nu' = 11$. A large fraction of the molecules fragments into $Li^+$ and Li upon ionization, which is observed when monitoring $Li^+$ for the same excitation spectrum (not shown).

The vertical bars in Figure 5b represent the transition for $J = 0$ rotational states starting from $\nu'' = 0$ in the $1^3\Sigma_u^+$ ground state as calculated with the potentials given in ref 32 by using the LEVEL 8.0 program of LeRoy.[53] The height of the bars reflects the calculated Franck–Condon (FC) distribution. Note that the use of a pulsed laser with relatively high pulse energy (~0.3 mJ), which is needed to ionize sufficient molecules in a one-color R2PI experiment, is not well suited for the determination of transition probabilities. Despite this disadvantage, the trend of the peak intensities reflects the trend in the calculated FC factors. The only exception is the relatively low intensity of the $\nu' = 0$ state when compared to the FC factor, which is most probably caused by saturation effects. Hence, we scale the FC factors to the $\nu' = 1$ peak (the FCF for $\nu' = 0$ is beyond the scale in Figure 5b). As can be seen in Figure 5, the origin of the rising edge of each peak matches the calculated values.

Alkali dimers are located on the surface of helium nanodroplets.[30] This represents a situation where a molecule is located on a two-dimensional superfluid. The vibronic bound–bound transitions with vibrationally resolved states typically consist of triangular shaped peaks, which have been analyzed for $Na_2$ in detail recently.[54,55] The rising edge of the peaks has its origin approximately (within a few wavenumbers) at the vibrational level of the free molecule. A small droplet induced shift on the order of a few wavenumbers was reported for $Na_2$ on helium droplets (e.g., −2.8 $cm^{-1}$ for the $1^1\Sigma_u^+$ ← $1^1\Sigma_g^+$ transition and +5 $cm^{-1}$ for the $1^3\Sigma_g^+$ ← $1^3\Sigma_u^+$ transition.[3,4]) Within the accuracy of our data, we can not exclude such a slight shift for the observed $Li_2$–$He_N$ transition. The vibrational band is broadened and extends to the high-frequency side. This broad wing is caused by the interaction of the excited electron of the molecule with the helium droplet, i.e., the excitation of phonons (phonon-wing). According to Bovino et al.,[30] the binding energies of $Li_2$ $1^1\Sigma_g^+$ and $Li_2$ $1^3\Sigma_u^+$ to a helium cluster of 30 atoms are of similar value around 50 $cm^{-1}$, but the positions at the surface differ significantly: while the intermolecular axis of the $Li_2$ $1^1\Sigma_g^+$ is oriented perpendicular to the surface, $Li_2$ $1^3\Sigma_u^+$ lies flat on the surface. For sodium dimers,[4] the singlet molecule spectra exhibit vibrational bands with narrow zero phonon lines and wide phonon-wings separated by a gap. In contrast, triplet spectra of $Na_2$ show a sharp rise at the onset of a vibrational band followed by a triangularly shaped phonon-wing without gap. This peculiar difference was theoretically analyzed by Tehver, Hizhnyakov, and Benedek.[54,55] The gapless appearance of a phonon-wing was attributed to a stronger coupling of vibrational motion of the dimer molecule to excitation modes of the helium droplet.

The recorded spectrum was fitted with a sum of asymmetric two-sigma functions[56]

$$\mathcal{L}(\bar{\nu}) = I(1 + e^{(\bar{\nu}-\bar{\nu}_0+w_1/2)/w_2})^{-1} [1 - (1 + e^{(\bar{\nu}-\bar{\nu}_0-w_1/2)/w_3})^{-1}] \quad (1)$$

We identify the position of the recorded peaks at the wavelength where the second derivative of eq 1 has a maximum for each set of fit parameters. This wavelength corresponds to the onset of the rising edge within a few wavenumbers (depending on the signal-to-noise ratio) and hence to the origin of the vibrational band. The results are compared to the calculated positions of the vibronic levels. The determined positions lie within an interval of 0 to +4 $cm^{-1}$ for $^7Li_2$ ($\nu' = 1-8$), −5 to +4 $cm^{-1}$ for $^6Li^7Li$ ($\nu' = 1-8$), and 0 to +11 $cm^{-1}$ for $^6Li_2$ ($\nu' = 1-4$) around each calculated value. Higher vibrational states and the $^6Li_2$–$He_N$ spectrum have a larger uncertainty due to the relatively low signal. The fit procedure does not reproduce accurately the calculated position of the origin of the $\nu' = 0$ level for $^7Li_2$ (the wavenumber for $^6Li^7Li$ differs by −12 $cm^{-1}$ from the calculated value). In this case, we identify the peak position with the onset of the rising edge at 21 707 $cm^{-1}$ (10 $cm^{-1}$ below the calculated value). The spectra in the upper panel in Figure 5 appear to be superimposed by a large nonresonant background signal, which reaches from 21 250 to 23 000 $cm^{-1}$. At the applied laser pulse energy, resonance enhanced two-photon ionization may be expected. According to ref 57, the ionization potential of free $Li_2$ lies at $T_e$ = 41 496 ± 4 $cm^{-1}$, and another $^7Li_2$ state, $2^3\Sigma_g^+$ ,may enhance the broad two-photon ionization signal.


dx.doi.org/10.1021/jp4030238 | J. Phys. Chem. A 2013, 117, 11866–11873

Experimental high resolution data and theoretical calculations are available for the $2^3\Pi_g$ state. This allows a detailed comparison between the spectroscopy of free molecules and molecules on the droplet. The most accurate experimental data have been obtained by perturbation facilitated optical−optical double resonance (PFOODR) spectroscopy,[31] where for the $2^3\Pi_g$ state all three isotopomers of the Li dimer have been investigated.[58−61] In order to use helium nanodroplets in future experiments as a matrix for the electronic spectroscopy of tailored molecules on their surface, we are interested in the accuracy of spectroscopic constants, which can be extracted from their spectra. Therefore, we determine the molecular constants for the sake of comparison with the literature values of free molecules. In Table 1, we summarize the molecular constants as obtained from a least-squares fit of the observed band positions to the standard expression[62]

$$T(v') = T + \omega_e\left(v' + \frac{1}{2}\right) - \omega_e x_e\left(v' + \frac{1}{2}\right)^2 \quad (2)$$

The obtained results are compared to experimental results from Xie and Field[58] (for $^6Li_2$) and Li et al.[61] (for $^7Li_2$). The parameters for $^6Li^7Li$ are calculated from the $^7Li_2$ parameter by a multiplication with the isotope factor[62] $\rho = (\mu^7/\mu)^{1/2}$, where $\mu^7$and $\mu$ are the reduced masses of $^7Li_2$ and $^6Li^7Li$, respectively. This is a valid approach within the Born−Oppenheimer approximation, where the three $Li_2$ isotopomers have identical potential curves. Although Born−Oppenheimer breakdown effects are significant in $Li_2$,[61] they can be neglected within the accuracy of our results. A direct determination of $T_e$ from our data is not possible since we only have access to the triplet molecule. Hence, we calculate $T_e$ from $T$ in eq 2 by adding a constant offset of 8213.8, 8215.2, and 8216.4 $cm^{-1}$ for $^7Li_2$, $^6Li^7Li$, and $^6Li_2$, respectively, which corresponds to the absolute energy of the $1^3\Sigma_u^+(v'' = 0)$ state.[63] The molecular parameters listed in Table 1 demonstrate that parameters deduced from lithium molecules on the surface of helium nanodroplets agree well with free molecule parameters (within the $2\sigma$ uncertainty interval).

## SUMMARY AND CONCLUSIONS

We have shown that two-photon spectroscopy of Li−$He_N$ offers a possibility to access Li−$He_N$ Rydberg states without UV lasers. We were able to assign the 3p ← 2s and 3d ← 2s transition of Li atoms on helium nanodroplets by using two different methods. Within the pseudodiatomic model, the states split into the 3P (Π,Σ) and 3D (Δ,Π,Σ) different molecular substates. The first approach (exciplex approach) used for the assignment exploits the fact that the exciplex formation process depends on the Λ quantum number of the intermediate state. In the second part of the discussion of Li−$He_N$, we present calculations for the description of the observed transitions. Li−$He_N$ potentials are generated by using a pairwise additive approach and assuming a frozen helium density that interacts with the excited dopant. The potential energy curves support the observed ordering of the states. The obtained Franck−Condon factors of the bound free transitions overestimate the blue shift of the transitions and reveal the necessity of more sophisticated theoretical models for the accurate description of excited Li−$He_N$ states, which are capable of including quantum effects,[14,24] which are non-negligible for lithium, as well as configuration interactions of the energetically close P and D states. As the lightest of the alkali metals, lithium is another interesting candidate for a detailed study of the corresponding alkali−$He_N$ Rydberg complex, so far investigated for Na−$He_N$,[16,17] Rb−$He_N$,[19,20] and Cs−$He_N$.[19,23] Recording the blue or red shifts of Rydberg states on droplets with respect to the free atom energies may provide further insight into the shielding effects of the helium droplet as obtained from our recent Rydberg−Ritz analysis.[19]

In addition to the spectroscopy of Li−$He_N$, we show for the first time a spectrum of a bound−bound transition of $Li_2$ molecules on the surface of $He_N$. The observed bands are identified as $2^3\Pi_g$ $(v')$ ← $1^3\Sigma_u^+$ $(v'' = 0)$ transitions. The REMPI-TOF technique allows to study all three isotopomers ($^6Li_2$, $^6Li^7Li$, and $^7Li_2$) of the Li dimer simultaneously. The spectrum comprises a series of vibronic transitions, broadened by the influence of the droplet. The vibronic transitions could be followed from $v' = 0$ to $v' = 11$ for the $^7Li_2$ isotope. Our investigation of $Li_2$ shows that despite the interaction between the molecule and the droplet, helium droplet isolation spectroscopy can serve as a tool to test ab initio molecular potentials of electronically excited states of species on the droplet surface. In future experiments, we plan to use our insights gained from the $Li_2$−$He_N$ experiments presented in this article and combine the Li atom with alkaline-earth atoms, a complex that can not be formed easily in the gas phase. Helium droplet isolation spectroscopy will provide a versatile tool to study these species and to test the corresponding ab initio potentials.

## AUTHOR INFORMATION

### Corresponding Author

*E-mail: florian.lackner@tugraz.at (F.L.); wolfgang.ernst@tugraz.at (W.E.E.).

### Notes

The authors declare no competing financial interest.

## ACKNOWLEDGMENTS

This research has been supported by the Austrian Science Fund (FWF) under Grant FWF-E-P19759 and the ERDF Program of the European Union and the Region of Styria.

## REFERENCES

(1) Callegari, C.; Ernst, W. E. Chapter: Helium Droplets as Nanocryostats for Molecular Spectroscopy - from the Vacuum Ultraviolet to the Microwave Regime In *Handbook of High-Resolution Spectroscopy*; Quack, M., Merkt, F.; John Wiley & Sons: Chichester, U.K., 2011; pp 1551−1594.

(2) Toennies, J. P.; Vilesov, A. F. Superfluid Helium Droplets: A Uniquely Cold Nanomatrix for Molecules and Molecular Complexes. *Angew. Chem., Int. Ed.* **2004**, *43*, 2622−2648.

(3) Stienkemeier, F.; Ernst, W. E.; Higgins, J.; Scoles, G. On the Use of Liquid Helium Cluster Beams for the Preparation and Spectroscopy of the Triplet States of Alkali Dimers and Other Weakly Bound Complexes. *J. Chem. Phys.* **1995**, *102*, 615−617.

(4) Higgins, J.; Callegari, C.; Reho, J.; Stienkemeier, F.; Ernst, W. E.; Gutowski, M.; Scoles, G. Helium Cluster Isolation Spectroscopy of Alkali Dimers in the Triplet Manifold. *J. Phys. Chem. A* **1998**, *102*, 4952−4965.

(5) Schulz, C. P.; Claas, P.; Schumacher, D.; Stienkemeier, F. Formation and Stability of High-Spin Alkali Clusters. *Phys. Rev. Lett.* **2004**, *92*, 013401.

(6) Theisen, M.; Lackner, F.; Ernst, W. E. Rb and Cs Oligomers in Different Spin Configurations on Helium Nanodroplets. *J. Phys. Chem. A* **2011**, *115*, 7005−7009.

(7) Hartmann, M.; Miller, R.; Toennies, J.; Vilesov, A. Rotationally Resolved Spectroscopy of $SF_6$ in Liquid Helium Clusters: A Molecular Probe of Cluster Temperature. *Phys. Rev. Lett.* **1995**, *75*, 1566−1569.
(8) Stienkemeier, F.; Higgins, J.; Callegari, C.; Kanorsky, S. I.; Ernst, W. E.; Scoles, G. Spectroscopy of Alkali Atoms (Li, Na, K) Attached to Large Helium Clusters. *Z. Phys. D* **1996**, *38*, 253−263.
(9) Brühl, F. R.; Trasca, R. A.; Ernst, W. E. Rb−He Exciplex Formation on Helium Nanodroplets. *J. Chem. Phys.* **2001**, *115*, 10220−10224.
(10) Auböck, G.; Nagl, J.; Callegari, C.; Ernst, W. E. Electron Spin Pumping of Rb Atoms on He Nanodroplets via Nondestructive Optical Excitation. *Phys. Rev. Lett.* **2008**, *101*, 035301.
(11) Bünermann, O.; Mudrich, M.; Weidemüller, M.; Stienkemeier, F. Spectroscopy of Cs Attached to Helium Nanodroplets. *J. Chem. Phys.* **2004**, *121*, 8880.
(12) Theisen, M.; Lackner, F.; Ernst, W. E. Cs Atoms on Helium Nanodroplets and the Immersion of $Cs^+$ Into the Nanodroplet. *J. Chem. Phys.* **2011**, *135*, 074306.
(13) Bünermann, O.; Droppelmann, G.; Hernando, A.; Mayol, R.; Stienkemeier, F. Unraveling the Absorption Spectra of Alkali Metal Atoms Attached to Helium Nanodroplets. *J. Phys. Chem. A* **2007**, *111*, 12684−12694.
(14) Hernando, A.; Mayol, R.; Pi, M.; Barranco, M.; Kerkines, I. S. K.; Mavridis, A. Li Atoms Attached to Helium Nanodroplets. *Int. J. Quantum Chem.* **2011**, *111*, 400−405.
(15) Scheidemann, A. A.; Kresin, V. V.; Hess, H. Capture of Lithium by $^4$He Clusters: Surface Adsorption, Penning Ionization, and Formation of $HeLi^+$. *J. Chem. Phys.* **1997**, *107*, 2839−2844.
(16) Loginov, E.; Drabbels, M. Unusual Rydberg System Consisting of a Positively Charged Helium Nanodroplet with an Orbiting Electron. *Phys. Rev. Lett.* **2011**, *106*, 083401.
(17) Loginov, E.; Callegari, C.; Ancilotto, F.; Drabbels, M. Spectroscopy on Rydberg States of Sodium Atoms on the Surface of Helium Nanodroplets. *J. Phys. Chem. A* **2011**, *115*, 6779−6788.
(18) Pifrader, A.; Allard, O.; Auböck, G.; Callegari, C.; Ernst, W. E.; Huber, R.; Ancilotto, F. One- and Two-Photon Spectroscopy of Highly Excited States of Alkali-Metal Atoms on Helium Nanodroplets. *J. Chem. Phys.* **2010**, *133*, 164502.
(19) Lackner, F.; Krois, G.; Ernst, W. E. Rydberg-Ritz Analysis and Quantum Defects for Rb and Cs Atoms on Helium Nanodroplets. *Mol. Phys.* **2013**, DOI: 10.1080/00268976.2013.788792.
(20) Lackner, F.; Krois, G.; Koch, M.; Ernst, W. E. Rubidium on Helium Droplets: Analysis of an Exotic Rydberg Complex for $n^* < 20$ and $0 \leq l \leq 3$. *J. Phys. Chem. Lett.* **2012**, *3*, 1404−1408.
(21) Theisen, M.; Lackner, F.; Ancilotto, F.; Callegari, C.; Ernst, W. E. Two-Step Excitation of Rb Atoms on He Nanodroplets. *Eur. Phys. J. D* **2011**, *61*, 403−408.
(22) Fechner, L.; Grüner, B.; Sieg, A.; Callegari, C.; Ancilotto, F.; Stienkemeier, F.; Mudrich, M. Photoionization and Imaging Spectroscopy of Rubidium Atoms Attached to Helium Nanodroplets. *Phys. Chem. Chem. Phys.* **2012**, *14*, 3843−3851.
(23) Lackner, F.; Krois, G.; Theisen, M.; Koch, M.; Ernst, W. E. Spectroscopy of nS, nP, and nD Rydberg Series of Cs Atoms on Helium Nanodroplets. *Phys. Chem. Chem. Phys.* **2011**, *13*, 18781−18788.
(24) Hernando, A.; Barranco, M.; Pi, M.; Loginov, E.; Langlet, M.; Drabbels, M. Desorption of Alkali Atoms From $^4$He Nanodroplets. *Phys. Chem. Chem. Phys.* **2012**, *14*, 3996−4010.
(25) Kramida, A. E.; Ralchenko, Y.; Reader, J.; Team, N. A. NIST Atomic Spectra Database (version 5.0), 2012; http://www.nist.gov/pml/data/asd.cfm.
(26) Auböck, G.; Nagl, J.; Callegari, C.; Ernst, W. E. Triplet State Excitation of Alkali Molecules on Helium Droplets: Experiments and Theory. *J. Phys. Chem. A* **2007**, *111*, 7404−7410.
(27) Brühl, F. R.; Miron, R. A.; Ernst, W. E. Triplet States of Rubidium Dimers on Helium Nanodroplets. *J. Chem. Phys.* **2001**, *115*, 10275−10281.
(28) Auböck, G.; Aymar, M.; Dulieu, O.; Ernst, W. E. Reinvestigation of the $Rb_2$ $(2)^3\Pi_g$−$a^3\Sigma_u^+$ Band on Helium Nanodroplets. *J. Chem. Phys.* **2010**, *132*, 054304.
(29) Ernst, W. E.; Huber, R.; Jiang, S.; Beuc, R.; Movre, M.; Pichler, G. Cesium Dimer Spectroscopy on Helium Droplets. *J. Chem. Phys.* **2006**, *124*, 024313.
(30) Bovino, S.; Coccia, E.; Bodo, E.; Lopez-Durán, D.; Gianturco, F. A. Spin-Driven Structural Effects in Alkali Doped $^4$He Clusters From Quantum Calculations. *J. Chem. Phys.* **2009**, *130*, 224903.
(31) Li, L.; Lyyra, A. Triplet States of $Na_2$ and $Li_2$ by Perturbation Facilitated Optical−Optical Double Resonance Spectroscopy. *Spectrochim. Acta* **1999**, *55*, 2147−2178.
(32) Jasik, P.; Sienkiewicz, J. Calculation of Adiabatic Potentials of $Li_2$. *Chem. Phys.* **2006**, *323*, 563−573.
(33) Nagl, J.; Auböck, G.; Hauser, A. W.; Allard, O.; Callegari, C.; Ernst, W. E. High-Spin Alkali Trimers on Helium Nanodroplets: Spectral Separation and Analysis. *J. Chem. Phys.* **2008**, *128*, 154320.
(34) Nagl, J.; Hauser, A. W.; Auböck, G.; Callegari, C.; Ernst, W. E. Optical Spectroscopy of Potassium-Doped Argon Clusters. Experiments and Quantum-Chemistry Calculations. *J. Phys. Chem. A* **2007**, *111*, 12386−12397.
(35) Lewerenz, M.; Schilling, B.; Toennies, J. A New Scattering Deflection Method for Determining and Selecting the Sizes of Large Liquid Clusters of $^4$He. *Chem. Phys. Lett.* **1993**, *206*, 381−387.
(36) Harms, J.; Toennies, J. P.; Dalfovo, F. Density of Superfluid Helium Droplets. *Phys. Rev. B* **1998**, *58*, 3341−3350.
(37) Edlen, B. Chapter Atomic Spectra. In *Handbuch der Phyik*; Flügge, S., Ed.; Springer: New York, 1964; , pp 80−220.
(38) Reho, J.; Callegari, C.; Higgins, J.; Ernst, W. E.; Lehmann, K. K.; Scoles, G. Spin−Orbit Effects in the Formation of the Na−-He Excimer on the Surface of He Clusters. *Faraday Discuss.* **1997**, *108*, 161−174.
(39) Dalfovo, F.; Lastri, A.; Pricaupenko, L.; Stringari, S.; Treiner, J. Structural and Dynamical Properties of Superfluid Helium: A Density-Functional Approach. *Phy. Rev. B* **1995**, *52*, 1193.
(40) Dalfovo, F.; Lehmann, K.; Schmied, R. Doped Clusters of $^4$He-Density Profiles and Energy, Trento, 1999. Modified 2000 in Princeton, 2007 Garching, 2012 Graz, written in FORTRAN; private communications.
(41) Schmied, R. Density-Functional Calculations of Excitations in Doped Helium Nanodroplets. Ph.D. thesis, Princeton University, 2005
(42) Poms, J.; Hauser, A. W.; Ernst, W. E. Helium Nanodroplets Doped With Xenon and Rubidium Atoms: a Case Study of van der Waals Interactions Between Heliophilic and Heliophobic Dopants. *Phys. Chem. Chem. Phys.* **2012**, *14*, 15158−15165.
(43) Patil, S. H. Adiabatic Potentials For Alkali Inert-Gas Systems in the Ground-State. *J. Chem. Phys.* **1991**, *94*, 8089−8095.
(44) Pascale, J. Use of l-Dependent Pseudopotentials in the Study of Alkali-Metal−Atom−He Systems. The Adiabatic Molecular Potentials. *Phys. Rev. A* **1983**, *28*, 632.
(45) Pascale, J. Adiabatic Potentials of Alkali−He Systems: Numerical Results. *Service de Physique des Atoms et des Surfaces*, 1983.
(46) Le Roy, R. J.; Kraemer, G. T. BCONT 2.2: A Computer Program for Calculating Bound−Continuum Transition Intensities for Diatomic Molecules. *Chemical Physics Research Report CP-650R2*; University of Waterloo: Canada, 2004.
(47) Dell'Angelo, D.; Guillon, G.; Viel, A. Excited Li and Na in $He_n$: Influence of the Dimer Potential Energy Curves. *J. Chem. Phys.* **2012**, *136*, 114308.
(48) Callegari, C.; Ancilotto, F. Perturbation Method to Calculate the Interaction Potentials and Electronic Excitation Spectra of Atoms in He Nanodroplets. *J. Phys. Chem. A* **2011**, *115*, 6789−6796.
(49) Müller, S.; Krapf, S.; Koslowski, T.; Mudrich, M.; Stienkemeier, F. Cold Reactions of Alkali-Metal and Water Clusters inside Helium Nanodroplets. *Phys. Rev. Lett.* **2009**, *102*, 183401.
(50) Hotta, S.; Doi, K.; Nakamura, K.; Tachibana, A. High-Spin Electronic Interaction of Small Lithium and Sodium Cluster Formation in the Excited States. *J. Chem. Phys.* **2002**, *117*, 142−152.

(51) an der Lan, L.; Bartl, P.; Leidlmair, C.; Schöbel, H.; Jochum, R.; Denifl, S.; Märk, T. D.; Ellis, A. M.; Scheier, P. The Submersion of Sodium Clusters in Helium Nanodroplets: Identification of the Surface → Interior Transition. *J. Chem. Phys.* **2011**, *135*, 044309.
(52) an der Lan, L.; Bartl, P.; Leidlmair, C.; Schöbel, H.; Denifl, S.; Märk, T. D.; Ellis, A. M.; Scheier, P. Submersion of Potassium Clusters in Helium Nanodroplets. *Phys. Rev. B* **2012**, *85*, 115414.
(53) Le Roy, R. J. LEVEL 8.0 a Computer Program for Solving the Radial Schrödinger Equation for Bound and Quasibound Levels. *Chemical Physics Research Report CP-663*; University of Waterloo: Canada, 2007.
(54) Hizhnyakov, V.; Tehver, I.; Benedek, G. Theory of the Optical Spectrum of $Na_2$ on $^4$He Droplets: Effects of the Zero-Point Energy of the Nearest Atoms. *Eur. Phys. J. B* **2009**, *70*, 507−512.
(55) Tehver, I.; Hizhnyakov, V.; Benedek, G. Sodium Molecule on the Surface of Liquid Helium-4 Droplets: Optical Transitions Probe Collective Excitations. *Phys. Status Solidi C* **2013**, *10*, 232−235.
(56) Auböck, G.; Nagl, J.; Callegari, C.; Ernst, W. E. Observation of Relativistic E x e Vibronic Coupling in $Rb_3$ and $K_3$ Quartet States on Helium Droplets. *J. Chem. Phys.* **2008**, *129*, 114501.
(57) Bernheim, R.; Gold, L.; Tipton, T.; Konowalow, D. The Ionization Potential of $^7Li_2$ and Bond Energy of $^7Li_2^+$. *Chem. Phys. Lett.* **1984**, *105*, 201−204.
(58) Xie, X.; Field, R. Perturbation Facilitated Optical−Optical Double Resonance Spectroscopy of the $^6Li_2$ $3^3\Sigma_g^+$, $2^3\Pi_g$, $1^3\Delta_g$, $b^2\Pi_g$ and $a^3\Sigma_u^+$ States. *J. Mol. Spectrosc.* **1986**, *117*, 228−244.
(59) Yiannopoulou, A.; Urbanski, K.; Antonova, S.; Lyyra, A. M.; Li, L.; An, T.; Whang, T. J.; Ji, B.; Wang, X. T.; Stwalley, W. C.; et al. The $2^3\Pi_g$ and $3^3\Pi_g$ States of $^7Li_2$: Optical−Optical Double Resonance Spectroscopy and ab Initio Calculations. *J. Chem. Phys.* **1995**, *103*, 5898−5903.
(60) Chen, D.; Li, L.; Wang, X.; Li, L.; Hui, Q.; Ma, H.; Li, L.; Xu, X.; Chun, D. Pulsed PFOODR Spectroscopy of Triplet Rydberg States of $^7Li_2$. *J. Mol. Spectrosc.* **1993**, *161*, 7−16.
(61) Li, D.; Xie, F.; Li, L.; Lazoudis, A.; Lyyra, A. M. New Observation of the $^6Li^7Li$ $3^3\Sigma_g^+$, $1^3\Delta_g$ and $2^3\Pi_g$ States and Molecular Constants With All $^6Li_2$, $^7Li_2$, and $^6Li^7Li$ Data. *J. Mol. Spectrosc.* **2007**, *246*, 180−186.
(62) Herzberg, G. *Molecular Spectra and Molecular Structure I. Spectra of Diatomic Moleules*; Van Nostrand Reinhold: New York, 1950.
(63) Xie, X.; Field, R. The Bound and Quasibound Levels of $^6Li_2$ $a^3\Sigma_u^+$. *J. Chem. Phys.* **1985**, *83*, 6193−6196.